Structure-Guided Design, Synthesis, and Evaluation of Salicylic Acid-Based Inhibitors Targeting a Selectivity Pocket in the Active Site of Human 20α-Hydroxysteroid Dehydrogenase (AKR1C1)

Ossama El-Kabbani,*,† Peter J. Scammells,† Joshua Gosling,† Urmi Dhagat,† Satoshi Endo,‡ Toshiyuki Matsunaga,‡ Midori Soda,‡ and Akira Hara‡

Medicinal Chemistry and Drug Action, Monash Institute of Pharmaceutical Sciences, 381 Royal Parade, Parkville, Victoria 3052, Australia, and Laboratory of Biochemistry, Gifu Pharmaceutical University, Mitahora-higashi, Gifu 502-8585, Japan

Received February 9, 2009

The first design, synthesis, and evaluation of human 20α-hydroxysteroid dehydrogenase (AKR1C1) inhibitors based on the recently published crystal structure of its ternary complex with inhibitor are reported. While the enzyme−inhibitor interactions observed in the crystal structure remain conserved with the newly designed inhibitors, the additional phenyl group of the most potent compound, 3-bromo-5-phenylsalicylic acid, targets a nonconserved hydrophobic pocket in the active site of AKR1C1 resulting in 21-fold improved potency (K_i = 4 nM) over the structurally similar 3α-hydroxysteroid dehydrogenase isoform (AKR1C2). The compound is hydrogen bonded to Tyr55, His117, and His222, and the phenyl ring forms additional van der Waals interactions with residues Leu308, Phe311, and the nonconserved Leu54 (Val in AKR1C2). Additionally, the metabolism of progesterone in AKR1C1-overexpressed cells was potently inhibited by 3-bromo-5-phenylsalicylic acid, which was effective from 10 nM with an IC_{50} value equal to 460 nM.

Introduction

Hydroxysteroid dehydrogenases (HSDs)[a] belong to two protein superfamilies, the aldo-keto reductase (AKR) superfamily[1] and the short-chain dehydrogenase/reductase superfamily.[2] Members of the AKR superfamily are NAD(P)(H)-dependent oxidoreductases that possess a triose phosphate isomerase (TIM) barrel motif consisting of an eight-stranded β-sheet at the core surrounded by eight α-helices.[3] While the four human HSDs belonging to the AKR1C subfamily, AKR1C1 (20α-HSD), AKR1C2 (type 3 3α-HSD), AKR1C3 (type 2 3α-HSD), and AKR1C4 (type 1 3α-HSD), share at least 86% sequence homology with AKR1C1 and AKR1C2 in particular differing only by seven residues, they display distinct positional and stereo preferences with respect to their substrates and are involved in different physiological roles.[4,5] AKR1C1 has a major role in progesterone metabolism that is essential for the maintenance of pregnancy.[6] The conversion of progesterone to an inactive progestin, 20α-hydroxyprogesterone, by AKR1C1 is associated with premature birth leading to infant morbidity and mortality.[7,8] AKR1C1 has been implicated in brain function where it modulates the occupancy of γ-aminobutyric acid type A ($GABA_A$) receptors through its reductive 20α-HSD activity, which converts neuroactive steroids (3α,5α-tetrahydroprogesterone and 5α-tetrahydrodeoxycorticosterone) and their precursors (5α-dihydroprogesterone and progesterone) into inactive and ineffective 20α-hydroxysteroids, thereby removing them from the synthetic pathway.[9,10] The elimination of neuroactive steroids by AKR1C1 is implicated in symptoms of premenstrual syndrome and other neurological disorders.[9,11] The enzyme is also involved in the development of several human and rodent tumors, such as lung, endometrial, esophageal, ovarian, and breast cancers, and its overexpression in cancer cells is related to drug-resistance against several anticancer agents.[12−16]

AKR1C1 is inhibited by a variety of compounds including bile acids, phytoestrogens, synthetic estrogens, benzodiazepines, nonsteroidal anti-inflammatory agents, and synthetic compounds.[10,17−21] Among the inhibitors, benzbromarone and 3′,3″,5′,5″-tetrabromophenolphthalein are the most potent inhibitors showing IC_{50} values of 48 and 33 nM, respectively.[10] Other inhibitors show IC_{50} or K_i values in the micromolar range, and either lack the selectivity to AKR1C1 or their selectivity was not examined using the four AKR1C isoforms. Recently, we have identified dihalogenated salicylic acid derivatives as potent inhibitors of AKR1C1 showing K_i values between 6−9 nM and determined the crystal structure of the first ternary complex with a potent inhibitor bound in the active site at 1.8 Å resolution.[22,23] The inhibitor 3,5-dichlorosalicylic acid was surrounded by side chains contributed by the 11 amino acid residues Tyr24, Leu54, Tyr55, Trp86, His117, His222, Glu224, Trp227, Leu306, Leu308, and Phe311 and anchored from its carboxylate group that formed hydrogen bonds with the catalytic residues His117 and Tyr55. Analysis of the inhibitor binding site revealed that four nonconserved residues (Leu54, His222, Leu306, and Leu308) in the four AKR1C isoforms are present within van der Waals contacts (<4.0 Å) from the inhibitor, and thus should be considered when designing specific inhibitors of AKR1C1. 3,5-Dichlorosalicylic acid shows a K_i value of 6 nM for AKR1C1 and greater than 4000-fold difference in inhibitor potency between AKR1C1 and the two isoforms AKR1C3 and AKR1C4, which is derived mainly from the nonconserved interactions between the inhibitor and residues Leu306 and Leu308 from the C-terminal loop.[23] The inhibitor also highly inhibits AKR1C2 that plays roles in the elimination of the potent androgen 5α-dihydrotestosterone and the synthesis of the $GABA_A$ receptor-modulated neuroactive steroids.[4,5,10] The high selectivity and similar potencies of the inhibitor for

* To whom correspondence should be addressed. Phone: 61-3-9903-9691. Fax: 61-3-9903-9582. E-mail: ossama.el-kabbani@pharm.monash.edu.au.
† Monash Institute of Pharmaceutical Sciences.
‡ Gifu Pharmaceutical University.

[a] Abbreviations: HSD, hydroxysteroid dehydrogenase; AKR, aldo-keto reductase; AKR1C1, human 20α-hydroxysteroid dehydrogenase; AKR1C2, human type 3 3α-hydroxysteroid dehydrogenase; *S*-tetralol, *S*-(+)-1,2,3,4-tetrahydro-1-naphthol; $GABA_A$, γ-aminobutyric acid type A; BAEC, bovine aortic endothelial cell; LC/MS, liquid chromatography/mass spectrometry.

10.1021/jm9001633 CCC: $40.75
Published on Web 04/27/2009

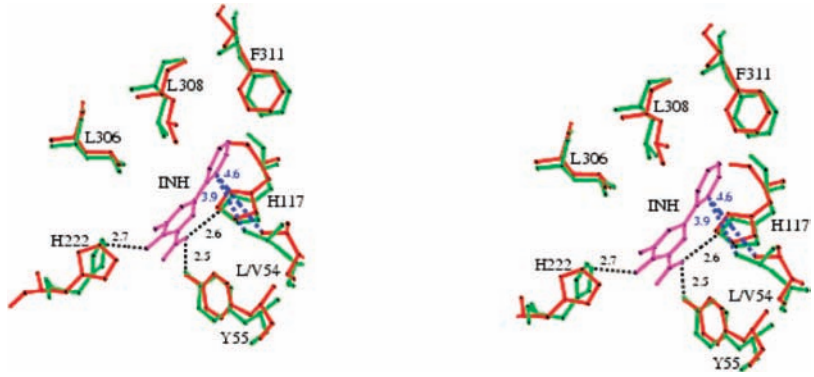

Figure 1. Stereoview of the inhibitor compound **4** (INH; pink color) modeled in the superimposed active sites of AKR1C1 (green color) and AKR1C2 (red color). The surrounding residues are labeled with their single letter code for clarity, and hydrogen bonds between the inhibitor and AKR1C1 are shown as black dotted lines with corresponding distances given in angstroms. The shortest contacts between the 5-phenyl moiety of the inhibitor and nonconserved residue 54 of AKR1C1 and AKR1C2 are shown in blue. The figure was prepared using *MOLSCRIPT*[34] after energy minimization.

Table 1. K_i Values of 3,5-Dibromosalicylic Acid (DBSA) and Compounds **4** and **9** for the AKR1C Isoforms

	K_i values (μM)			
inhibitor	AKR1C1	AKR1C2	AKR1C3	AKR1C4
DBSA	0.009 ± 0.0002	0.082 ± 0.0023 (9)[a]	23 ± 1.1 (2600)	45.7 ± 5.9 (5100)
compound **4**	0.004 ± 0.0004	0.087 ± 0.012 (21)	4.2 ± 0.15 (890)	18.2 ± 2.5 (3900)
compound **9**	0.14 ± 0.017	1.97 ± 0.013 (14)	21 ± 3.4 (150)	NI[b]

[a] Ratios of AKR1C isoforms (1C2-1C4) to AKR1C1 are given in parentheses. [b] No inhibition was observed at inhibitor concentrations upto 100 μM.

AKR1C1 and AKR1C2 are due to the homologous structures of their active sites that differ by only one amino acid residue, which is Leu54 in AKR1C1 and is Val54 in AKR1C2.[23] Thus, it is important that newly designed inhibitors capture the maximum interactions with Leu54 of AKR1C1 in order to improve the selectivity over AKR1C2.

In this study, we report the first design, synthesis, and evaluation of AKR1C1 inhibitors based on the recently published crystal structure of the AKR1C1 ternary complex.[23] While the enzyme−inhibitor interactions observed in the crystal structure remain conserved with the newly designed inhibitors, the additional phenyl group of the most potent compound, 3-bromo-5-phenylsalicylic acid (K_i = 4 nM), targets a hydrophobic pocket in the active site of AKR1C1 interacting with the nonconserved Leu54, resulting in improved specificity over AKR1C2. In addition, this compound potently inhibited the metabolism of progesterone by AKR1C1 in the cells, showing an IC_{50} (concentration for 50% inhibition of this metabolism) value of 460 nM. These results provide the framework needed for the development of new inhibitors that are more specific to AKR1C1 for potential use in treatments against cancer and neurological disorders.

Results and Discussion

The crystal structure of AKR1C1[23] together with a GRID[24] analysis of the inhibitor-binding site suggested that the replacement of the bromine atom at the 5-position of 3,5-dibromosalicylic acid with a phenyl (compound **4**) is expected to enhance the inhibitor potency and selectivity for AKR1C1 over AKR1C2. Benzene rings and other aromatic systems are common moieties among compounds used as therapeutic agents, playing major roles ranging from providing steric bulk to forming an integral part of the pharmacophore.[25] Residues present within van der Waals contacts of the modeled compound **4** are shown in Figure 1. The carboxyl and hydroxyl groups of this compound are hydrogen bonded to the side-chains of Tyr55, His117, and His222, and its phenyl moiety enters a hydrophobic selectivity pocket forming additional van der Waals interactions with residues Leu308, Phe311, and the nonconserved Leu54 (Val in AKR1C2). As previously observed in the structure of the ternary complex,[23] the salicylic acid moiety is present with van der Waals contacts from Leu306. In addition to the synthesis of compound **4**, 3-phenyl-5-bromosalicylic acid (compound **9**) that has the phenyl and bromo groups present at opposite positions compared to that in compound **4**, was synthesized for comparison, and together with 3,5-dibromosalicylic acid, the inhibitory potencies of the three compounds were measured against the four isoforms (AKR1C1 to AKR1C4). With the exception of compound **9** and AKR1C4, the three compounds inhibited the four isoforms competitively with respect to the substrate *S*-(+)-1,2,3,4-tetrahydro-1-naphthol (*S*-tetralol), and their K_i values are shown in Table 1. Compound **9** showed the least potency for AKR1C1 and AKR1C2, likely due to short contacts and disruption of the hydrogen bonding interaction with His222 (Figure 1). However, compound **4** showed improved potency and selectivity toward AKR1C1 compared to those of 3,5-dibromosalicylic acid because of the additional favorable interactions between the 5-phenyl ring and the residues lining the selectivity pocket (Figure 1), and was a 21-fold more potent inhibitor of AKR1C1 than AKR1C2. Additionally, compared to 3,5-dichlorosalicylic acid,[23] compound **4** displayed a 2.9-fold enhancement in the calculated binding energies of the AKR1C1−inhibitor complex (−114 kcal/mol vs −39 kcal/mol) and was a 2-fold more potent and selective inhibitor of AKR1C1 than AKR1C2.

Chemical Synthesis of Compounds 4 and 9. Compound **4** was synthesized using the approach outlined in Scheme 1. Briefly, this involved a Suzuki coupling between methyl 5-iodosalicylate (**1**) and phenyl boronic acid to give the biphenyl **2**. Bromination of the 3-position (Br_2) followed by saponification of the methyl ester ($LiOH.H_2O$) afforded the target compound **4** in good yield (75% over two steps).

The synthetic approach of compound **9** is depicted in Scheme 2. Methyl 5-bromosalicylate was reacted with NaI and chloram-

Scheme 1. Synthesis of 3-Bromo-5-phenylsalicylic Acid (**4**)[a]

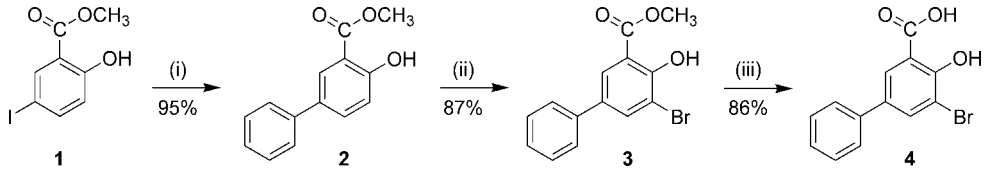

[a] Reagents and conditions: (i) $PhB(OH)_2$, K_2CO_3, $Pd(PPh_3)_4$, DMF, 70 °C, 24 h; (ii) Br_2, MeOH, rt, 20 min; (iii) $LiOH.H_2O$, $THF:H_2O$ (4:1), 70 °C, 24 h.

Scheme 2. Synthesis of 3-Phenyl-5-bromosalicylic Acid (**9**)[a]

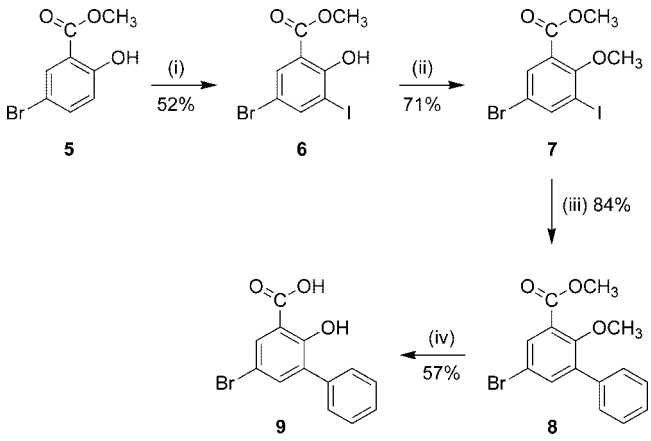

[a] Reagents and conditions: (i) NaI, Chloramine T, DMF, rt; (ii) MeI, K_2CO_3, DMF, rt; (iii) $PhB(OH)_2$, K_3PO_4, $Pd(PPh_3)_4$, DMF, 100 °C; (iv) BBr_3 (1 M in CH_2Cl_2), CH_2Cl_2, −78 °C.

ine T to give the corresponding 3-iodo analogue **6**. Suzuki coupling of this compound with phenyl boronic acid did not proceed cleanly (by TLC); therefore, it was decided to first protect the phenol as the corresponding methyl ether **7**. This straightforward transformation was achieved using methyl iodide and potassium carbonate. Coupling of methyl 2-methoxy-3-iodo-5-bromobenzoate (**7**) with phenyl boronic acid afforded the desired biphenyl **8** in 84% yield. The reaction of **8** with excess boron tribromide effected the cleavage of both the methyl ether and ester to yield the target compound, 5-bromo-3-phenylsalicylic acid (**9**).

Bovine aortic endothelial cells (BAECs) that are transfected with the cDNA for AKR1C1 were used to evaluate the inhibitory potency of 3,5-dibromosalicyclic acid, compound **4**, and compound **9** at the cellular level. The expression of AKR1C1 in the cells was confirmed by assaying the *S*-tetralol dehydrogenase activity. The activity in the extract of the transfected cells (0.27 unit/mg) was 10-fold higher than that of the control cells transfected with the vector alone. This was also evident in the metabolism of progesterone in the transfected cells (Figure 2), but not in the control cells. The transfected BAECs metabolized progesterone only into 20α-hydroxyprogesterone as shown in the liquid chromatography/mass spectrometry (LC-MS) chromatogram (Figure 2a), where the retention time of this metabolite was identical to that of authentic 20α-hydroxyprogesterone and distinct from that (16 min) of authentic 20*β*-hydroxyprogesterone. Compound **9**, compound **4**, and 3,5-dibromosalicylic acid inhibited the metabolism of progesterone in the cells, as shown in the representative LC-MS chromatogram for the addition of compound **4** (Figure 2b). Comparison of the dose−response curves for the three inhibitors (Figure 3) indicated that compound **4** most potently inhibited the metabolism of progesterone. It was effective from 10 nM, and the IC_{50} value was 460 nM. 3,5-Dibromosalicylic acid was effective from 0.1 μM, and its IC_{50} value was 2.3 μM, while the inhibition by

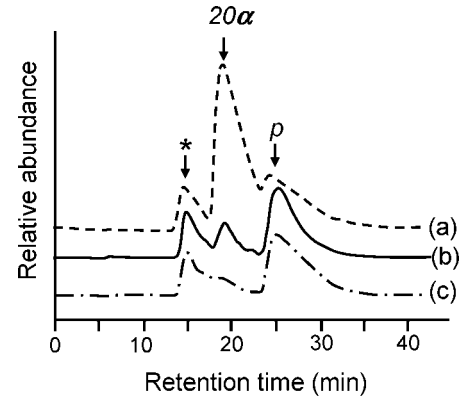

Figure 2. LC/MS analysis of the metabolism of progesterone (*p*) in control and AKR1C1-overexpressed BAECs. The cells were cultured for 6 h in the medium containing 30 μM progesterone in the absence or presence of 10 μM compound **4**. Chromatograms: (a) the overexpressed cells incubated without inhibitor, (b) the overexpressed cells incubated with compound **4**, and (c) the control cells without inhibitor. The position of the metabolite was identical to that of the authentic 20α-hydroxyprogesterone (20α). The peak other than that of the substrate and metabolite is due to unknown substances (*), which are present in the medium.

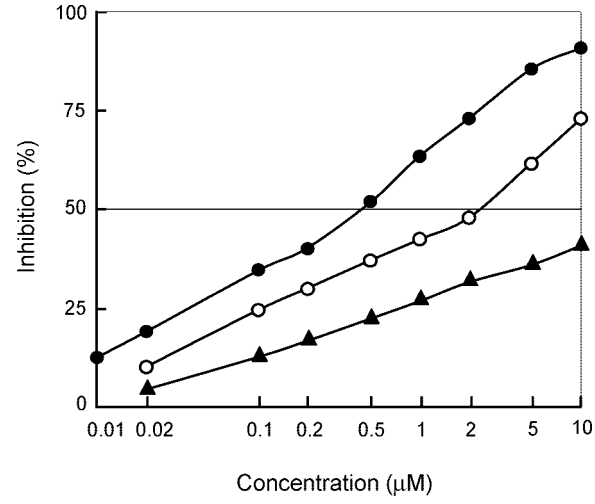

Figure 3. Dose−response curves for 3,5-dibromosalicylic acid, compound **4**, and compound **9** in the inhibition of progesterone metabolism by the AKR1C1-overexpressed BAECs. (○), 3,5-dibromosalicylic acid; (▲), compound **9**; and (●), compound **4**. The cell culture conditions were the same as those described in the legend of Figure 2.

compound **9** was low, as evident by only 40% inhibition at its high concentration of 10 μM. It should be noted that the three compounds did not affect the cell viability up to their concentrations of 10 μM. The ratio of the IC_{50} value of compound **4** to that of 3,5-dibromosalicylic acid was 5, which is higher than the ratio of K_i values of the two compounds for AKR1C1. This suggests that the addition of the phenyl ring at 5-position of

the salicylic acid resulted in increasing the cell permeability of the inhibitor.

In summary, the use of the recently determined crystal structure of AKR1C1 complexed with an inhibitor in conjunction with a GRID analysis of the inhibitor-binding site has allowed the design of a new salicylic acid-based inhibitor (compound **4**) with improved potency (K_i = 4 nM) and selectivity (21-fold) over that of AKR1C2. Moreover, compound **4** significantly decreased the metabolism of progesterone in the cells with an IC_{50} value of 460 nM, which is comparable or superior to the IC_{50} values of the previously known two most potent inhibitors of AKR1C1, benzbromarone and 3′,3″,5′,5″-tetrabromophenolphthalein.[10] Compound **4** was designed to target a selectivity pocket in the active site of AKR1C1 lined by the three apolar residues Leu54, Leu308, and Phe311. Leu308 is one of two nonconserved C-terminal residues (the other residue is Leu306) responsible for the greater than 4000-fold difference in inhibitor potency between AKR1C1 and the two isoforms AKR1C3 and AKR1C4.[23] Since the active sites of AKR1C1 and AKR1C2 differ only by one amino acid residue, which is Leu54 in AKR1C1 and is Val54 in AKR1C2, and the current inhibitors show similar potency for the two enzymes, newly designed inhibitors that capture the maximum interactions with Leu54 in AKR1C1 are needed in order to improve their selectivity over AKR1C2. Thus, future developments of new derivatives of compound **4** are likely to improve on the selectivity of the currently known AKR1C1 inhibitors. We have also illustrated that while large chemical database searches are useful in discovering new enzyme inhibitors, the use of the high resolution crystal structure of an enzyme−inhibitor complex is an effective tool in optimizing the enzyme−inhibitor interaction by exploiting the small structural differences between the different enzyme isoforms.

Experimental Section

Molecular Modeling and Inhibitor Design. In an attempt to develop potent and more specific inhibitors of the enzyme, compounds were designed based on the crystal structure of the AKR1C1 ternary complex.[23] To aid the design process, the program GRID[24] (version 18) was used to search the active site of the enzyme for the most suitable or favorable positions of a variety of probes, as previously described by our laboratory for L-xylulose reductase.[26] Briefly, a total of 25 probes were tested with AKR1C1, which included the following groups: methyl, aromatic carbon, amino, amido, and heterocyclic nitrogens, halogens, sulfur, carbonyl, ether, and hydroxyl oxygen, carboxy group, water, phosphate, and other ions. Each probe was analyzed independently using the InsightII 2.1 package (Biosym Technologies Inc., San Diego, CA). Calculations were performed on a cube (35 Å per side) centered on the active site, with a grid spacing of 0.5 Å. The interaction energy between the probe and every atom within the protein structure was evaluated at each grid point. A dielectric constant of 80 was used to simulate a bulk aqueous phase, while areas as determined by GRID to be excluded from solvent were assigned a dielectric constant of 4 (i.e., the interior of the protein). The accompanying program GRIN was used to automatically assign atom types and charges for the protein, using the standard parameter file provided with GRID. The output was converted (using GINS supplied with GRID) into a form suitable for input to the Biosym utility contour, and contour maps were built up using steps of 1 kcal/mol. The contour map detailed a number of energy levels. Negative energy levels delineate regions at which ligand binding is favored in particular, and positive energy levels define the surface of the target. The contour map was then superimposed on the active site of AKR1C1 using InsightII. Visual inspection of the superimposed 3,5-dichlorosalicylic acid on the active site of AKR1C1 provided information on the predicted position of the probe with respect to the inhibitor. The most favored probe suggested by the program that may improve the binding and specificity of the 3,5-dihalogenated salicylic acids to AKR1C1 over AKR1C2 was the phenyl because of its binding in a hydrophobic pocket and interaction with the nonconserved Leu54 (Val in AKR1C2).

3-Bromo-5-phenylsalicylic acid (compound **4**) was manually docked into the active site of AKR1C1, on the basis of the observed orientation of 3,5-dicholorosalicylic acid in the 1.8 Å resolution crystal structure,[23] and any water molecules in the active site coinciding with the docked compound were removed. While there was no apparent steric hindrance in the model of the complex, to relieve any strain associated with the crystal coordinates the model was subjected to energy minimization using the Discover 2.7 program (Biosym Technologies, San Diego, California, USA) on a Linux workstation following published protocols found to be effective for visualizing a protein−ligand complex in its lowest energy conformation.[27,28] Briefly, hydrogen atoms, partial charges, atomic potentials, and bond orders were assigned by using the automatic procedures within InsightII. Arginine, lysine, aspartate, and glutamate amino acids were charged, while histidines were uncharged, with hydrogen atoms fixed at the Nε2 atoms. Energy minimization calculations included a constant-valence force field incorporating the simple harmonic function for bond stretching and excluding all nondiagonal terms were carried out (cutoff distance of 26 Å) using the steepest-descent and conjugate-gradient algorithms (down to a maximum atomic root-mean-square derivative of 10.0 kcal/Å and 0.01 kcal/Å, respectively). Additionally, the values for the intermolecular binding energy were calculated for the enzyme−inhibitor complexes with 3,5-dichlorosalicylic acid and compound **4** bound in the active site using Discover as previously described.[26]

Chemistry. NMR spectra were recorded on a Bruker 300 WB spectrometer with an Avance console. Unless otherwise stated, ^{1}H and ^{13}C NMR spectra were obtained in $CDCl_3$ at 300 and 75 MHz, respectively. High-resolution electrospray mass spectra (HRMS) were obtained on a Waters LCT Premier XE (TOF) spectrometer. TLC analyses were run on precoated silica gel 60 F_{254} aluminum plates (Merck), and compounds were analyzed under UV light and stained using phosphomolybdic acid (48 g in 100 mL of EtOH). Column chromatography was performed using Merck silica gel 60 (particle size 0.063−0.200 μm, 70−230 mesh). The purity of the target compounds (**4** and **9**) was determined to be >98% by LC-MS using an Agilent 6120 Quadrapole LC-MS with an Eclipse XDB-C18 column (5 μm, 4.6 × 150 mm).

Methyl 5-phenylsalicylate (2). Methyl 5-iodosalicylate (**1**) (0.150 g, 0.539 mmol) was dissolved in anhydrous, degassed DMF (5 mL). Potassium phosphate tribasic (0.240 g, 1.131 mmol), $Pd(PPh_3)_4$ (0.035 g, 0.003 mmol, 5 mol %), and phenyl boronic acid (0.073 g, 0.599 mmol) were added, and the reaction mixture was stirred at 70 °C overnight. The reaction mixture was partitioned between CH_2Cl_2 (30 mL) and H_2O (50 mL), and the aqueous layer was further extracted with CH_2Cl_2 (2 × 10 mL). The combined organic phase were dried (Na_2SO_4), filtered, and reduced *in vacuo* to give brown crystals (0.128 g, 96%). ^{1}H NMR δ 4.00 (m, 3H), 7.09 (d, 1H, J = 8.7, 1H), 7.36 (t, 1H, J = 7.5 Hz), 7.46 (t, 2H, J = 7.5 Hz), 7.58 (d, 2H, J = 8.4 Hz), 7.72 (d, 1H, 2.4, 8.4 Hz), 8.11 (d, 1H, J = 2.4 Hz), 10.75 (s, 1H).

Methyl 3-Bromo-5-phenylsalicylate (3). Methyl 5-phenylsalicylate (**2**) (0.198 g, 0.86 mmol) was dissolved in MeOH (5 mL), and a solution of Br_2 (50 μL, 0.97 mmol) in MeOH (2 mL) was added dropwise. The reaction mixture was stirred overnight at room temperature. A precipitate formed during the course of the reaction and was collected via vacuum filtration and washed with cold MeOH (0.02 g, 87%). ^{1}H NMR δ 4.02 (s, 3H), 7.36 (d, 1H, J = 7.2 Hz), 7.45 (br t, 2H, J = 7.5 Hz), 7.54 (d, 2H, J = 7.5 Hz), 7.99 (d, 1H, J = 2.1 Hz), 8.06 (d, 1H, J = 2.1 Hz), 11.45 (s, 1H).

3-Bromo-5-phenylsalicylic Acid (4). Methyl 3-bromo-5-phenylsalicylate (**3**) (0.120 g, 0.387 mmol) was dissolved in THF/H_2O (4:1) (4 mL), $LiOH\cdot H_2O$ (0.081 g, 1.937 mmol) added, and the reaction refluxed overnight. The reaction was diluted with water and acidified to pH 1 with 5 M HCl (5 mL). Extraction with CH_2Cl_2

(4 × 5 mL) followed by drying (Na_2SO_4), filtration, and evaporation afforded a white solid (0.098 g, 86%). ^{1}H NMR δ 7.35 (d, 1H, J = 7.2 Hz), 7.47 (d, 2H, J = 7.2 Hz), 7.55 (d, 2H, J = 7.2 Hz), 8.05 (d, 1H, J = 2.3 Hz), 8.13 (d, 1H, J = 2.3 Hz), 11.2 (s, 1H). ^{13}C NMR δ 112.3, 115.9, 127.6, 128.7, 128.8, 130.3, 133.6, 137.6, 139.0, 158.4, 172.8. HRMS (ESI) m/z cacld for $C_{13}H_9BrO_3$ [M − H]$^-$: 290.9662. Found: 290.9654.

Methyl 3-iodo-5-bromosalicylate (6). Methyl 5-bromosalicylate (**5**) (15.00 g, 64.92 mmol) was dissolved in DMF (50 mL) prior to the addition of NaI (11.68 g, 77.92 mmol) followed by chloramine T (20.60 g, 77.03 mmol). The reaction mixture was stirred overnight at room temperature. After filtration and evaporation of the solvent, the resultant residue was taken up in Et_2O (250 mL) and washed with H_2O (5 × 100 mL), $Na_2S_2O_3$ (100 mL), and brine (100 mL). The Et_2O layer was separated, dried, and evaporated to give a yellow solid, which was recrystallized from EtOH (12.50 g, 52%). ^{1}H NMR δ 3.99 (s, 3H), 7.98 (d, 1H, J = 2.4 Hz), 8.05 (d, 1H, J = 2.4 Hz), 11.55 (s, 1H).

Methyl 2-methoxy-3-iodo-5-bromobenzoate (7). Methyl 3-iodo-5-bromosalicylate (**6**) (0.98 g, 2.74 mmol) was dissolved in DMF (5 mL), and potassium carbonate (0.53 g, 3.73 mmol) and iodomethane (0.24 mL, 3.86 mmol) were added. The reaction mixture was stirred at ambient temperature overnight prior to being diluted with Et_2O (20 mL) and washed with H_2O (5 × 100 mL). The organic layer was dried (Na_2SO_4), filtered, and evaporated *in vacuo* to give a yellow solid (0.55 g, 54%). ^{1}H NMR δ 3.89 (s, 3H), 3.94 (s, 3H), 7.92 (d, 1H, J = 2.4 Hz, 1H), 8.07 (d, 1H, J = 2.4 Hz).

Methyl 5-bromo-2-methoxybiphenyl-3-carboxylate (8). Methyl 5-bromo-3-iodo-2-methoxybenzoate (**7**) (0.150 g, 0.40 mmol) was dissolved in degassed DMF (8 mL), and tribasic potassium phosphate (0.103 g, 0.485 mmol), tetrakis(triphenylphosphine)-palladium (0.025 g, 0.002 mmol), and phenylboronic acid (0.06 g, 0.492 mmol) were added. The reaction mixture was stirred overnight at 100 °C. After cooling to room temperature, the solution was diluted with CH_2Cl_2 (10 mL) and washed with water (10 mL). The aqueous layer was acidified with 5 M HCl (5 mL) and extracted with CH_2Cl_2 (3 × 10 mL). The combined organic extracts were dried (Na_2SO_4), filtered, and reduced *in vacuo*, and the resultant residue was purified by column chromatography using hexane/CH_2Cl_2 (2:1) eluent to afford the target compounds as a brown solid (0.087 g, 89% yield). ^{1}H NMR δ 3.47 (s, 3H), 3.95 (s, 3H), 7.38−7.56 (m, 5H), 7.62 (d, 1H, J = 2.7 Hz), 7.87 (d, 1H, J = 2.7 Hz).

3-Phenyl-5-bromosalicylic Acid (9). Methyl 5-bromo-2-methoxybiphenyl-3-carboxylate (**8**) (0.13 g, 0.39 mmol) was dissolved in dry CH_2Cl_2 (3 mL) under N_2. The solution was cooled to −78 °C in a dry ice/acetone bath, and boron tribromide (0.67 mL, 0.98 mmol) was added dropwise. After stirring overnight in a dry ice/acetone bath, the reaction mixture was diluted with CH_2Cl_2 (10 mL) and washed with 1 M citric acid (2 × 30 mL) and saturated $NaHCO_3$ (30 mL). The aqueous layer was cooled on ice and acidified with 5 M HCl (10 mL). A white precipitate formed and was collected by vacuum filtration (0.07 g, 57%). ^{1}H NMR δ 7.36−7.47 (m, 3H), 7.56 (d, 2H, J = 7.8 Hz), 7.66 (d, 1H, J = 2.4 Hz), 8.03 (d, 1H, J = 2.4 Hz), 11.10 (s, 1H). ^{13}C NMR δ 111.2, 112.8, 128.2, 128.4, 129.3, 132.2, 133.0, 135.5, 140.3, 158.7, 173.5. HRMS (ESI) m/z cacld for $C_{13}H_9BrO_3$ [M − H]$^-$: 290.9662. Found: 290.9662.

Enzyme and Activity Assays. The recombinant AKR1C1, AKR1C2, AKR1C3, and AKR1C4 were expressed in *Escherichia coli* JM109 and purified to homogeneity as previously described.[29−31] Protein concentration was determined by a bicinchoninic acid protein assay reagent kit (Pierce) using bovine serum albumin as the standard. The NADP$^+$-linked *S*-tetralol dehydrogenase activity of the enzymes was assayed by measuring the rate of change in NADPH fluorescence (at 455 nm with an excitation wavelength of 340 nm) or its absorbance (at 340 nm) at 25 °C, as described previously.[23] In the inhibition assays, the IC_{50} values for the inhibitors were initially determined with the *S*-tetralol concentration (0.1 mM for AKR1C1 and 1 mM for other enzymes) using a software ED_{50} and IC_{50} for graded Response version 1.2. The inhibition patterns were determined by fitting the initial velocities using five substrate concentrations (0.2−2 × K_m for AKR1C3 and 0.5−5 × K_m for other enzymes) in the presence of the inhibitor concentrations (0−0.5 × IC_{50}) to Lineweaver−Burk and Dixon plots. The K_i values were calculated by using the appropriate programs of ENZFITTER (Biosoft, Cambrige, UK) and are expressed as the mean ± standard error of at least three determinations.

Evaluation of Inhibitors in the Cells. BAECs, a generous gift from Taisho Pharmaceutical Co. (Saitama, Japan), were cultured in Dulbecco's modified Eagle's medium supplemented with 10% fetal bovine serum, penicillin (100 U/mL), and streptomycin (100 μg/mL) at 37 °C in a 5% CO_2 incubator. In all experiments, the cells were used at passages 4−8, and the endothelial cobblestone morphology was confirmed microscopically before use. The expression vector with the cDNA for AKR1C1 was constructed according to the method previously reported.[32] The cDNA was initially amplified from the bacterial expression vector pGEX/AKR1C1[29] by PCR using the primer pairs consisting of a forward primer (5′-GA*GTCGAC*gccacc<u>ATG</u>GATTCGAAATATCAGTGT-3′) and a reverse primer (5′-AG*GTCGAC*<u>TTA</u>TATTCATCAGAAAATGGA-3′), in which *Sal*I site, a Kozak sequence and a start codon are expressed in italic letters, small letters, and underlined letters, respectively. The PCR product was verified by automated DNA sequencing and subcloned at the *Sal*I site of the eukaryotic expression vector pGW1.[32] The expression vector with the insert was then transfected into subconfluent BAECs using Lipofectamine 2000 (Invitrogen). The transfected cells were maintained in the medium containing 2% fetal bovine serum for 24 h and then used to evaluate the inhibitory effects of 3,5-dibromosalicylic acid and compounds **4** and **9** on the metabolism of progesterone in the cells. The cells were pretreated for 2 h with various concentrations of inhibitors in serum-free growth medium prior to incubating for 6 h with 30 μM progesterone. The culture media were collected by centrifugation, and the lipidic fraction of the media was extracted twice by ethyl acetate. The metabolite, 20α-hydroxyprogesterone, was quantified on a LC-MS using a Chiralcel OJ-H 5 μm column as described previously.[33]

Acknowledgment. U.D. is the recipient of a Monash Graduate School postgraduate scholarship. This work was partly supported by a Grant-in-Aid for Young Scientists (to S.E.).

References

(1) Hyndman, D.; Bauman, D. R.; Heredia, V. V.; Penning, T. M. The aldo-keto reductase superfamily homepage. *Chem. Biol. Interact.* **2003**, *143*−*144*, 621–631.
(2) Oppermann, U.; Filling, C.; Hult, M.; Shafqat, N.; Wu, X.; Lindh, M.; Shafqat, J.; Nordling, E.; Kallberg, Y.; Persson, B.; Jörnvall, H. Short-chain dehydrogenases/reductases (SDR): the 2002 update. *Chem. Biol. Interact.* **2003**, *143*−*144*, 247–253.
(3) Jez, J. M.; Bennett, M. J.; Schlegel, B. P.; Lewis, M.; Penning, T. M. Comparative anatomy of the aldo-keto reductase superfamily. *Biochem. J.* **1997**, *326*, 625–636.
(4) Penning, T. M.; Burczynski, M. E.; Jez, J. M.; Hung, C. F.; Lin, H. K.; Ma, H.; Moore, M.; Palackal, N.; Ratnam, K. Human 3α-hydroxysteroid dehydrogenase isoforms (AKR1C1-AKR1C4) of the aldo-keto reductase superfamily: functional plasticity and tissue distribution reveals roles in the inactivation and formation of male and female sex hormones. *Biochem. J.* **2000**, *351*, 67–77.
(5) Bauman, D. R.; Steckelbroeck, S.; Penning, T. M. The roles of aldo-keto reductases in steroid hormone action. *Drug News Perspect.* **2004**, *17*, 563–578.
(6) Zhang, Y.; Dufort, I.; Rheault, P.; Luu-The, V. Characterization of a human 20α-hydroxysteroid dehydrogenase. *J. Mol. Endocrinol.* **2000**, *25*, 221–228.
(7) Lewis, M. J.; Wiebe, J. P.; Heathcote, J. G. Expression of progesterone metabolizing enzyme genes (AKR1C1, AKR1C2, AKR1C3, SRD5A1, SRD5A2) is altered in human breast carcinoma. *BMC Cancer* **2004**, *4*, 27–39.
(8) Piekorz, R. P.; Gingras, S.; Hoffmeyer, A.; Ihle, J. N.; Weinstein, Y. Regulation of progesterone levels during pregnancy and parturition by signal transducer and activator of transcription 5 and 20α-hydroxysteroid dehydrogenase. *Mol. Endocrinol.* **2005**, *19*, 431–440.

(9) Lambert, J. J.; Belelli, D.; Hill-Venning, C.; Peters, J. A. Neurosteroids and GABAA receptor function. *Trends Pharmacol. Sci.* **1995**, *16*, 295–303.
(10) Higaki, Y.; Usami, N.; Shintani, S.; Ishikura, S.; El-Kabbani, O.; Hara, A. Selective and potent inhibitors of human 20α-hydroxysteroid dehydrogenase (AKR1C1) that metabolizes neurosteroids derived from progesterone. *Chem. Biol. Interact.* **2003**, *143*−*144*, 503–513.
(11) Eser, D.; Schüle, C.; Baghai, T. C.; Romeo, E.; Uzunov, D. P.; Rupprecht, R. Neuroactive steroids and affective disorders. *Pharmacol. Biochem. Behav.* **2006**, *84*, 656–666.
(12) Wiebe, J. P. Role of progesterone metabolites in mammary cancer. *J. Dairy Res.* **2005**, *72*, 51–57.
(13) Deng, H. B.; Adikari, M.; Parekh, H. K.; Simpkins, H. Ubiquitous induction of resistance to platinum drugs in human ovarian, cervical, germ-cell and lung carcinoma tumor cells overexpressing isoforms 1 and 2 of dihydrodiol dehydrogenase. *Cancer Chemother. Pharmacol.* **2004**, *54*, 301–307.
(14) Wang, H. W.; Lin, C. P.; Chiu, J. H.; Chow, K. C.; Kuo, K. T.; Lin, C. S.; Wang, L. S. Reversal of inflammation-associated dihydrodiol dehydrogenases (AKR1C1 and AKR1C2) overexpression and drug resistance in nonsmall cell lung cancer cells by wogonin and chrysin. *Int. J. Cancer* **2007**, *120*, 2019–2027.
(15) Rizner, T. L.; Smuc, T.; Rupreht, R.; Sinkovec, J.; Penning, T. M. AKR1C1 and AKR1C3 may determine progesterone and estrogen ratios in endometrial cancer. *Mol. Cell. Endocrinol.* **2006**, *248*, 126–135.
(16) Selga, E.; Noé, V.; Ciudad, C. J. Transcriptional regulation of aldo-keto reductase 1C1 in HT29 human colon cancer cells resistant to methotrexate: role in the cell cycle and apoptosis. *Biochem. Pharmacol.* **2008**, *75*, 414–426.
(17) Brozic, P.; Cesar, J.; Kovac, A.; Davies, M.; Johnson, A. P.; Fishwick, C. W.; Lanisnik Rizner, T.; Gobec, S. Derivatives of pyrimidine, phthalimide and anthranilic acid as inhibitors of human hydroxysteroid dehydrogenase AKR1C1. *Chem. Biol. Interact.* **2009**, *178*, 158–164.
(18) Brozic, P.; Turk, S.; Lanisnik Rizner, T.; Gobec, S. Discovery of new inhibitors of aldo-keto reductase 1C1 by structure-based virtual screening. *Mol. Cell. Endocrinol.* **2009**, *301*, 245–250.
(19) Byrns, M. C.; Penning, T. M. Type 5 17β-hydroxysteroid dehydrogenase/prostaglandin F synthase (AKR1C3): role in breast cancer and inhibition by non-steroidal anti-inflammatory drug analogs. *Chem. Biol. Interact.* **2009**, *178*, 221–227.
(20) Brozic, P.; Smuc, T.; Gobec, S.; Rizner, T. L. Phytoestrogens as inhibitors of the human progesterone metabolizing enzyme AKR1C1. *Mol. Cell. Endocrinol.* **2006**, *259*, 30–42.
(21) Usami, N.; Yamamoto, T.; Shintani, S.; Ishikura, S.; Higaki, Y.; Katagiri, Y.; Hara, A. Substrate specificity of human 3(20)α-hydroxysteroid dehydrogenase for neurosteroids and its inhibition by benzodiazepines. *Biol. Pharm. Bull.* **2002**, *25*, 441–445.
(22) Dhagat, U.; Carbone, V.; Chung, R. P.; Matsunaga, T.; Endo, S.; Hara, A.; El-Kabbani, O. A salicylic acid-based analogue discovered from virtual screening as a potent inhibitor of human 20α-hydroxysteroid dehydrogenase. *Med. Chem.* **2007**, *3*, 546–550.
(23) Dhagat, U.; Endo, S.; Sumii, R.; Hara, A.; El-Kabbani, O. Selectivity determinants of inhibitor binding to human 20α-hydroxysteroid dehydrogenase: Crystal structure of the enzyme in ternary complex with coenzyme and the potent inhibitor 3,5-dichlorosalicylic acid. *J. Med. Chem.* **2008**, *51*, 4844–4848.
(24) Goodford, P. J. A computational procedure for determining energetically favorable binding sites on biologically important macromolecules. *J. Med. Chem.* **1985**, *28*, 849–857.
(25) Lednicer, D. *Strategies for Organic Drug Synthesis and Design*; Wiley-Inter science: New York, 1998; pp 31−32.
(26) Carbone, V.; Ishikura, S.; Hara, A.; El-Kabbani, O. Structure-based discovery of human L-xylulose reductase inhibitors from database screening and molecular docking. *Bioorg. Med. Chem.* **2005**, *13*, 301–312.
(27) Darmanin, C.; El-Kabbani, O. Modelling studies on the binding of substrate and inhibitor to the active site of human sorbitol dehydrogenase. *Bioorg. Med. Chem. Lett.* **2000**, *10*, 1101–1104.
(28) Darmanin, C.; El-Kabbani, O. Modelling studies of the active site of human sorbitol dehydrogenase: an approach to structure-based inhibitor design of the enzyme. *Bioorg. Med. Chem. Lett.* **2001**, *11*, 3133–3136.
(29) Matsuura, K.; Hara, A.; Deyashiki, Y.; Iwasa, H.; Kume, T.; Ishikura, S.; Shiraishi, H.; Katagiri, Y. Roles of the C-terminal domains of human dihydrodiol dehydrogenase isoforms in the binding of substrates and modulators: probing with chimaeric enzymes. *Biochem. J.* **1998**, *336*, 429–436.
(30) Matsuura, K.; Shiraishi, H.; Hara, A.; Sato, K.; Deyashiki, Y.; Ninomiya, M.; Sakai, S. Identification of a principal mRNA species for human 3α-hydroxysteroid dehydrogenase isoform (AKR1C3) that exhibits high prostaglandin D_2 11-ketoreductase activity. *J. Biochem.* **1998**, *124*, 940–946.
(31) Shiraishi, H.; Ishikura, S.; Matsuura, K.; Deyashiki, Y.; Ninomiya, M.; Sakai, S.; Hara, A. Sequence of the cDNA of a human dihydrodiol dehydrogenase isoform (AKR1C2) and tissue distribution of its mRNA. *Biochem. J.* **1998**, *334*, 399–405.
(32) Tanaka, N.; Aoki, K.; Ishikura, S.; Nagano, M.; Imamura, Y.; Hara, A.; Nakamura, K. T. Molecular basis for peroxisomal localization of tetrameric carbonyl reductase. *Structure* **2008**, *16*, 388–397.
(33) Ishikura, S.; Nakajima, S.; Kaneko, T.; Shintani, S.; Usami, N.; Yamamoto, I.; Carbone, V.; El-Kabbani, O.; Hara, A. Comparison of Stereoselective Reduction of 3- and 20-Oxosteroids among Mouse and Primate 20α-Hydroxysteroid Dehydrogenases. In *Enzymology and Molecular Biology of Carbonyl Metabolism 12*; Weiner, H., Plapp, B., Lindahl, R., Maser, E., Eds.; Purdue University Press: West Lafayette, IN, 2005; pp 341−351.
(34) Kraulis, P. MOLSCRIPT: a program to produce both detailed and schematic plots of protein structures. *J. Appl. Crystallogr.* **1991**, *24*, 946–950.

JM9001633